Full length article

Vorinostat and Simvastatin have synergistic effects on triple-negative breast cancer cells via abrogating Rab7 prenylation

Xinhui Kou[a], Yonghua Yang[a,*], Xiaoxiao Jiang[a], Huijuan Liu[a], Fanghui Sun[a], Xuan Wang[a], Longkai Liu[a], Hongrui Liu[a], Zhaohu Lin[b], Lan Jiang[c]

[a] Department of Pharmacology and Biochemistry, School of Pharmacy, Fudan University, 826 Zhangheng Road, Shanghai 201203, China
[b] Chemical Biology, Roche Pharmaceutical Research and Early Development, Roche Innovation Center Shanghai, 720 Cailun Road, Shanghai 201203, China
[c] Department of Biological Sciences, Oakland University, 2200 N. Squirrel Road, Rochester, MI 48309, USA

ABSTRACT

Since the lack of targeted treatment, triple-negative breast cancer (TNBC) has poor outcomes. Histone deacetylase inhibitors (HDACi) blocking the activity of specific HDACs have emerged as cancer therapeutic agents. However, the therapeutic efficiency is still not satisfactory for patients with solid tumor. We thus performed screening for the synergistic agents of Vorinostat (SAHA). The resulting candidate Simvastatin was obtained. The efficacy and mechanism of combination have been studied in TNBC cells. The synergism of SAHA and Simvastatin was evaluated by IC_{50} of proliferation and combination index (CI). The antitumor activities of combination were further evaluated in TNBC cells. The pro-apoptotic effects were determined by flow cytometry and Western blot. Autophagosome-lysosome fusion was monitored using confocal microscope. The underlying mechanism was further studied by over-expressing of wild-type or inactive (C205S/C207S) Rab7 in compounds treated cells. The in vivo efficacy was also evaluated in mice. The combination of SAHA and Simvastatin had potent synergism in apoptosis of TNBC cells. It exerted pro-apoptosis effect by compromising the fusion between autophagosome and lysosome. Over-expressing of wild-type, but not inactive Rab7 rescued cells from apoptosis induced by the combinatory treatments. Mevalonate supplementation also decreased the combinatory treatment-induced apoptosis. These results indicate that the combinatory treatment enhances the apoptosis of TNBC cells by interrupting Rab7 prenylation and obstructing autophagosome-lysosome fusion. Combination between SAHA and Simvastatin could also significantly decrease the tumor growth in xenografted mice by inducing apoptosis and inhibiting Rab7 prenylation. Rab7 is a potential target for the combined effects of Simvastatin and SAHA.

1. Introduction

Breast cancer with high mortality is considered as the second leading cause of cancer-related deaths among women in the United States, and 255,180 new diagnoses are expected in 2017 (Giuliano et al., 2017). Several targeted therapies are available for breast cancers over-expressing either hormone receptors or growth-promoting protein HER2 (Giuliano et al., 2017). However, there is about ~ 20% of breast cancers are triple negative (TNBC) (Bianchini et al., 2016; Lehmann et al., 2011). TNBC lacking targeted therapies, have the poorest overall prognosis compared with other breast cancer types (Blows et al., 2010). Thus new approaches are remained to be developed for TNBC treatment. Histone deacetylase inhibitors (HDACi) have attracted more and more attentions in the recent clinical trials for therapy of TNBC (Chiu et al., 2016; Schech et al., 2015; Tate et al., 2012).

Suberoylanilide hydroxamic acid (Vorinostat, SAHA) depresses the de-acetylating activity of all 11 known human class I and class II HDACs (Grant et al., 2007), and shows moderate inhibition on TNBC cells (Palmieri et al., 2009). It not only induces apoptosis of TNBC cells via caspase activation and poly ADP-ribose polymerase (PARP) cleavage, but also exhibits potent cell growth inhibition and cell-cycle arrest in cancer cells (Deming et al., 2014; Schelman el al, 2013; Zibelman et al., 2015).

Autophagy allows the degradation and recycling of cellular materials. Cancer cells up-regulate autophagy under cellular stress to facilitate chemotherapeutic resistance (Mowers et al., 2016; Wei et al., 2014; Dupere-Richer et al., 2013). Autophagosome-lysosome fusion is a critical stage of autophagy mediated by the late endosome-/lysosome-associated small GTPase Rab7 (Wang et al., 2011; Wen et al., 2017). Failure of autophagosome-lysosome fusion causes the accumulation of

malfunctioning proteins in cells, impairs the recycling of materials and energy, and thus exerts cytotoxic effects (Gandesiri et al., 2012). Autophagy is becoming an attractive target to enhance the proficiency of existing cancer treating strategy (Dupere-Richer et al., 2013). Unfortunately, SAHA is an inducer of autophagy. It may weaken its anti-tumor activity (Dupere-Richer et al., 2013), and agents blocking autophagic flux may have synergism with SAHA in cancer treatment (Patel et al., 2016; Torgersen et al., 2013).

The present study identified that Simvastatin, a well-known 3-hydroxy-3-methylglutaryl-coenzyme A reductase (HMGCR) inhibitor of mevalonate pathway (Åberg et al., 2008; Gopalan et al., 2013), could enhance the pro-apoptotic effect of SAHA on TNBC via interrupting Rab7 prenylation and autophagosome-lysosome fusion.

2. Material and methods

2.1. Cells and culture conditions

TNBC cell lines MDA-MB-231, MDA-MB-468, and MDA-MB-453 were cultured in RPMI-1640 medium (Wisent, Canada) containing 10% fetal bovine serum (FBS, Gibco, Australia). TNBC cell line Hs578T and non-malignant fibrocystic disease cell line MCF-10A were maintained in DMEM (Wisent, Canada) supplemented with 10% FBS. All cell lines were obtained from the American Type Culture Collection (ATCC). Cells were grown at 37 °C in a humidified incubator with 95% air and 5% CO_2.

2.2. Chemicals and reagents

Dimethyl sulfoxide (DMSO), SAHA, Simvastatin, Mevastatin, and Pravastatin were purchased from Selleck Chem (Houston, USA). LOPAC1280 library (#LO3300, 1280 compounds, with each 10 µmol/l in stock) was purchased from Sigma-Aldrich (St. Louis, USA). Cell Counting Kit-8 (CCK8) was obtained from Dojindo Molecular Tech (Kumamoto, Japan). Annexin V-FITC and propidium iodide (PI) was obtained from BD Biosciences (San Jose, USA). RNeasy Mini Kit was purchased from QIAGEN (San Jose, USA). Lipofectamine 2000 transfection reagent and LysoTracker Blue was purchased from Life technologies (Paisley, UK). RevertAid First Strand cDNA Synthesis Kit and Maxima SYBR Green/Fluorescein qPCR Master Mix Kit were purchased from Thermo Fisher (Waltham, USA). The cDNA encoding mRFP-GFP-LC3 (tfLC3) and mRFP-LC3 were derived from ptfLC3 (Addgene) and sub-cloned into the lentiviral vector, pCDH-MCS-EF-puro (System Bioscience). The cDNA encoding Rab7 was produced from total HEK293 RNA by using RevertAid First Strand cDNA Synthesis Kit and sub-cloned into the lentiviral vector, pCDH1-MCS1-EF1-puro.

2.3. Determination of proliferative IC_{50}

Cells were seeded in 96-well plates at 1×10^4 cells/well and incubated with increasing concentrations of compounds for 72 h. Empty wells and wells treated with DMSO were used as blank and control, respectively. Cells were then allowed to incubate with CCK8 reagent for another 2 h, and the absorbance at 450 nm was quantified using a Tecan M200Pro microplate reader (Tecan, Austria). For calculating proliferative IC_{50}, the proliferative inhibition rate (IR) of each compound was calculated by using the formula: IR_1 (%) = $(OD_{control} - OD_{compound})/(OD_{control} - OD_{blank}) \times 100\%$; and the IR of each compound in combination with 0.5 µmol/l SAHA was calculated by IR_2 (%) = $(OD_{SAHA} - OD_{compound})/(OD_{SAHA} - OD_{blank}) \times 100\%$. Prism 5.0 software (California, USA) was employed for IC_{50} calculation by non-linear regression method.

2.4. Determination of combination index (CI)

Cells were seeded in 96-well plates at 1×10^4 cells/well, and were

Table 1
Compounds to have synergism with SAHA on MDA-MB-231.

Cell lines	Screening hits	IC_{50} µmol/l	IC_{50}, with 0.5 µmol/l SAHA
MDA-MB-231	Ellipticine	8.65 ± 0.42	1.53 ± 0.07[a]
	Mevastatin	9.28 ± 0.82	1.61 ± 0.08[a]
	Tyrphostin A9	> 60	9.86 ± 0.31[a]
	DEDA	> 60	6.78 ± 0.28[a]

MDA-MB-231 cells were treated with compounds (LOPAC1280 library) alone or in combination with SAHA (0.5 µmol/l) for 72 h. Proliferative IC_{50} of each compound either alone or in the presence of SAHA were calculated. Screening hits were identified as to significantly increase the anti-proliferative activity of compounds alone. Experiments were performed in triplicate, and data were presented as the mean ± S.E.M.. Statistical analysis was performed by using student's *t*-test.

[a] $P < 0.01$ as compared with cells in the presence of each compound alone.

treated with Simvastatin and/or SAHA (both from 32 to 0.03 µmol/l, serial 2-fold dilutions) for 72 h. Empty wells and wells treated with DMSO were used as blank and control, respectively. Cells were then allowed to incubate with CCK8 reagent for another 2 h, and the absorbance at 450 nm was quantified using a Tecan M200Pro microplate reader (Tecan, Austria). For calculating CI, the IR of each compound either alone or with SAHA was calculated by using the formula: IR_1 (%) = $(OD_{control} - OD_{compound})/(OD_{control} - OD_{blank}) \times 100\%$. Calcusyn 2.0 software (Cambridge, UK) was employed for CI calculation, The synergism was evaluated by CI in ED_{25}, ED_{50}, ED_{75}, and ED_{90}. A CI value of < 1, $= 1$, or > 1 indicates synergistic, additive, or antagonistic effects, respectively.

2.5. Screening of candidates in combination with SAHA

MDA-MB-231 cells were seeded in 96-well plates at 1×10^4 cells/well, and incubated with compounds (LOPAC1280 library) alone or in combination with SAHA (0.5 µmol/l) for 72 h. Proliferative IC_{50} of each compound either alone or with SAHA were calculated as described above. Hits were identified as to significantly increase the anti-proliferative activity of compounds alone in MDA-MB-231 cells.

2.6. Apoptosis analysis

MDA-MB-231 and MDA-MB-468 cells were seeded in 6-well plates at 5×10^5 cells/well, and treated with SAHA, Simvastatin, or SAHA plus Simvastatin for 24 h. Cells were collected and treated with PI (50 µg/ml final concentration) and 100:1 annexin V avoiding light for 10 min at room temperature. Stained cells were subjected to FACS procedure, and data were processed with CellQuest software.

2.7. Western blot

MDA-MB-231 and MDA-MB-468 cells were seeded in 60-mm dish, and treated with SAHA, Simvastatin, or SAHA plus Simvastatin for 24 h. Cells were collected and lysed by NP-40 lysis buffer (25 mmol/l Tris-HCl, pH 7.6, 150 mmol/l NaCl, 1 mmol/l EDTA, 1% NP-40) supplemented with protease inhibitor cocktail (#78430) from Pierce. Protein concentrations were quantified by using Bradford reagent. 20–30 µg proteins per sample was subjected to SDS-PAGE separation, and transferred onto nitrocellulose membranes followed by blotting with antibodies. Blots were recorded onto films by employing enhanced chemiluminescence from Millipore.

Primary antibodies against Caspase8 (#9746), Caspase3 (#9662), Caspase9 (#9502), PARP1 (#9542), Bid (#2002), Bcl-2 (#2870), Bcl-xL (#2762), Bax (#5023), Rab7 (#9367), LC3A/B (#4108), SQSTM1 (#5114), NBR1 (#9891), NDP52 (#9036), and β-actin (#4967) were purchased from Cell Signaling Technology. Secondary antibodies anti-Rabbit-HRP and anti-Mouse-HRP were from Jackson ImmunoResearch.
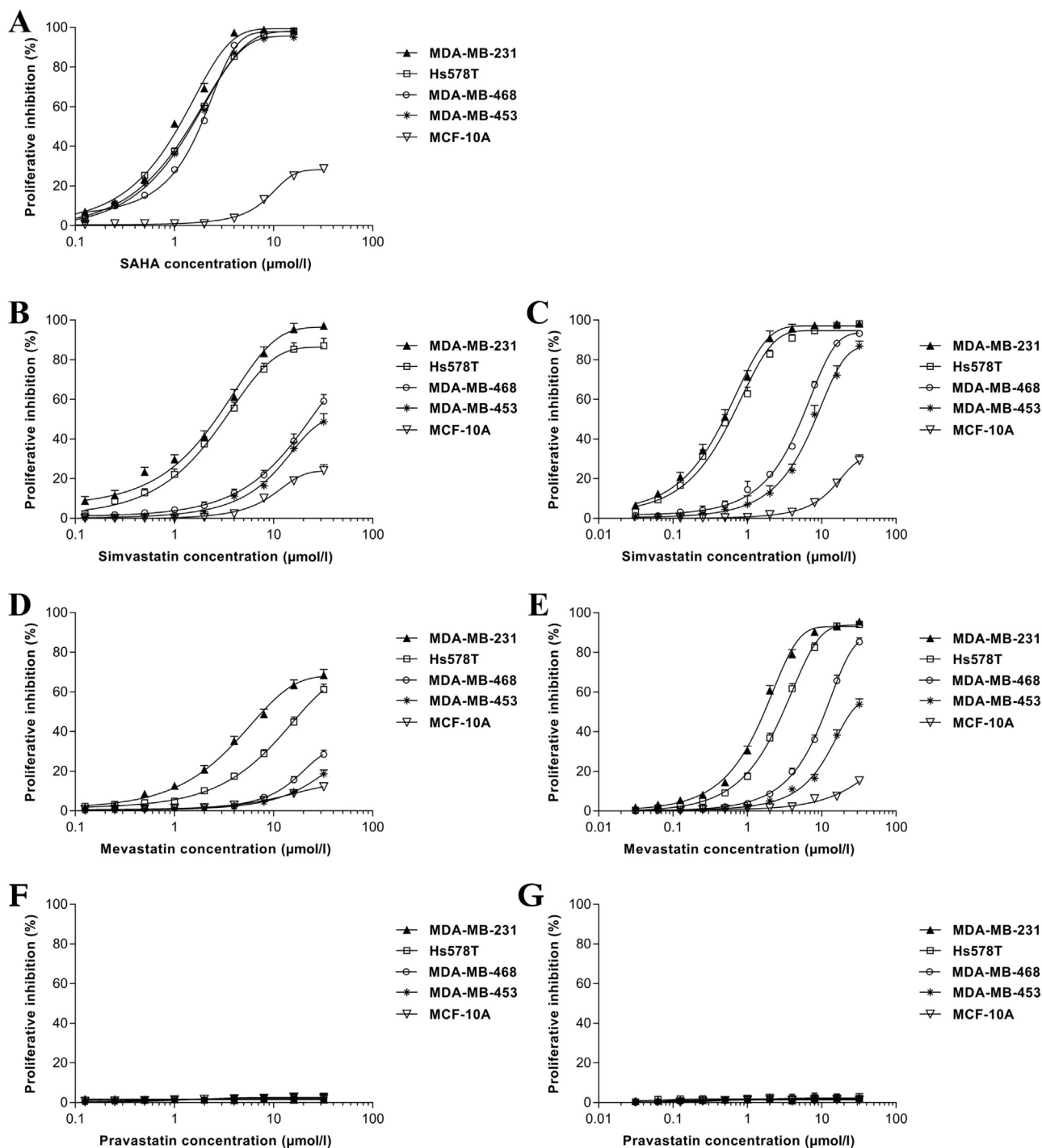
Fig. 1. The effects of SAHA and Statins on the proliferation of TNBC cells. TNBC or MCF-10A cells were treated with (A) SAHA, (B) Simvastatin, (C) Simvastatin plus 0.5 μmol/l SAHA, (D) Mevastatin, (E) Mevastatin + 0.5 μmol/l SAHA, (F) Pravastatin, and (G) Pravastatin plus 0.5 μmol/l SAHA. Except for that a final concentration of 0.5 μmol/l SAHA was used in combination groups, serial 2-fold dilutions of each compound in a final concentration range of 32–0.03 μmol/l were used in experiments. Cell counting was assessed by using CCK8 reagent at 72 h after treatments. Dose-response curves were plotted as concentration (logarithmic scale) versus normalized response – variable slope using non-linear regression by software Prism 5.0 (Graphpad). Experiments were performed in triplicate, and data were presented as the mean ± S.E.M.

2.8. Quantitative-PCR

Cells or tissues were lysed, and total RNA were extracted with RNeasy Mini Kit, followed by reverse transcription with RevertAid First Strand cDNA Synthesis Kit. Real-Time PCR was performed using Maxima SYBR Green qPCR Master Mix in PIKOREAL 96 Real-Time PCR System. The profile of thermal cycling consisted of initial denaturation at 95 °C for 10 min, and 40 cycles at 95 °C for 10 s and 60 °C for 30 s,

and 55 °C rise to 95 °C for melt curves. All primers used for qPCR analysis were synthesized by Invitrogen. The specificity of each primer pair was confirmed by melting curve analysis and agarose-gel electrophoresis. GAPDH was used as an internal control. Sequences of primers for SQSTM1, forward: 5′-GCACCCCAATGTGATCTGC-3′, reverse: 5′-CGCTACACAAGTCGTAGTCTGG-3′; GAPDH, forward: 5′-GGAGCGAG ATCCCTCCAAAAT-3′, reverse: 5′- GGCTGTTGTCATACTTCTCATGG-3′.

Table 2
IC$_{50}$ of compounds on the proliferation of TNBC cells with or without SAHA.

Breast cancer cell lines	SAHA	Simvastatin	Simvastatin + 0.5 μmol/l SAHA	Mevastatin	Mevastatin + 0.5 μmol/l SAHA
	μmol/l				
MDA-MB-231	0.99 ± 0.07	2.19 ± 0.31	0.42 ± 0.03[a]	9.28 ± 0.82	1.61 ± 0.08[b]
Hs578T	1.32 ± 0.10	3.16 ± 0.20	0.54 ± 0.02[a]	20.03 ± 0.78	2.84 ± 0.09[b]
MDA-MB-468	1.61 ± 0.18	23.61 ± 0.99	4.94 ± 0.39[a]	> 60	10.67 ± 0.36[b]
MDA-MB-453	1.40 ± 0.11	31.79 ± 2.47	7.99 ± 0.35[a]	> 60	26.97 ± 1.53[b]

TNBC cells were treated with distinct compounds. Except for that a final concentration of 0.5 μmol/l SAHA was used in combination groups, serial 2-fold dilutions of each compound in a final concentration range of 32–0.03 μmol/l were used in experiments. Cell counting was assessed by using CCK8 reagent at 72 h after treatments. Proliferative IC$_{50}$ were calculated by software Prism 5.0 (Graphpad) using non-linear regression, concentration (logarithmic scale) versus normalized response – variable slope. Experiments were performed in triplicate, and data were presented as the mean ± S.E.M. Statistical analysis was performed by using student's t-test.

[a] $P < 0.01$ as compared with cells in the presence of Simvastatin alone.
[b] $P < 0.01$ as compared with cells in the presence of Mevastatin alone.

2.9. Transfection and lentivirus package

To produce the lentivirus, three plasmid DNAs (pCDH: psPAX2: pMD2G = 4:3:1) were transfected into HEK293T cells using lipofectamine 2000 reagent according to the manufacturer's instructions. After 6 h, the original medium was replaced with fresh medium, and the lentiviral supernatant was collected 48 and 72 h later.

2.10. MDA-MB-231 stable cell line and confocal microscopy

Recombinant lentivirus encoding either tfLC3 or mRFP-LC3 were produced by HEK293T cells to infected MDA-MB-231 cells, and 1 μg/ml of puromycin (Invitrogen) was used to select for stable cells that express tfLC3 or mRFP-LC3. Images were acquired with an LSM710 confocal microscope with a 63 × oil objective (Carl Zeiss).

2.11. Animal xenograft evaluation

MDA-MB-231 cells were in situ injected into fat pad of immunocompromised BALB/c nu/nu mice (5- to 6-week old females, Fudan University, China). All animal procedures and maintenance were conducted in accordance with the protocols approved by the Institutional Animal Care and Use Committee at Fudan University. Tumors were measured, and volume was calculated by equation: $V = 0.5 \times \text{width}^2 \times \text{length}$. When tumor volume reached nearly 100 mm^3, mice were assigned into four groups randomly, and each group contained at least 5 mice. Groups were named as control (vehicle treatment), SAHA (20 mg/kg/day, orally), Simvastatin (10 mg/kg/day, orally), and combination (SAHA + Simvastatin) groups. After the initiating of treatment, measurements of tumor volume were performed by digital valipers every 5 days. Body weights were also monitored every 5 days. Group mean body weights loss of less than 20% and not more than one treatment-related death among treating groups during compound administration were defined as acceptable toxicity.

2.12. TUNEL assay

TUNEL assay was performed by employing In situ cell death detection kit and following the manufacturer's protocol from Roche. Briefly, slides were washed twice with PBS. After drying areas around the sample, 50 μl TUNEL reagents were added. After incubation, samples were further washed with PBS for three times. Nuclei were stained by DAPI reagent before confocal microscopy detection.

2.13. Statistical analysis

Data were obtained from 3 independent experiments, if not explicitly described in the figure legend, and presented as mean ± S.E.M. Statistical analysis was performed by using Prism 5.0 (student's t-test, one-way ANOVA, or two-way ANOVA). $P < 0.05$ was considered as statistically significant.

3. Results

3.1. The inhibition of TNBC cells by SAHA and Simvastatin

SAHA had moderate inhibitory effect on several TNBC cells. To find out whether other agents could enhance its efficacy, we employed chemicals from LOPAC library as combination partners to study the anti-proliferation activity. Four active compounds were identified to have synergistic effects with SAHA on MDA-MB-231 (Table 1). Among them, it is interesting that Mevastatin is synergistic with SAHA in antitumor effect. Thus we also tested the IC$_{50}$ values of other two statins, Simvastatin and Pravastatin besides Mevastatin. Either used alone or in combination with SAHA. TNBC cell lines used in the study showed similar IC$_{50}$ to SAHA treatment (MDA-MB-231: 0.99 μmol/l, Hs578T: 1.32 μmol/l, MDA-MB-468: 1.61 μmol/l, and MDA-MB-453: 1.40 μmol/l) (Fig. 1A). Compared with other statins, Simvastatin had most potent anti-proliferative effects on those TNBC cells. The IC$_{50}$ values for single use were 2.19, 3.16, 23.61, and 31.79 μmol/l in MDA-MB-231, Hs578T, MDA-MB-468, and MDA-MB-453 cells, respectively (Fig. 1B). When combined with SAHA, IC$_{50}$ values were 0.42, 0.54, 4.94, and 7.99 μmol/l in MDA-MB-231, Hs578T, MDA-MB-468, and MDA-MB-453 cells, respectively (Fig. 1C), significantly lower than values of Simvastatin used alone (Fig. 1B). Mevastatin had relatively weaker anti-proliferative activity than Simvastatin, either for single use or combination (Fig. 1D and E). The IC$_{50}$ values were listed in Table 2. Pravastatin had little antitumor effect (Fig. 1F and G). MCF-10A, non-malignant cells, was not affected much by Simvastatin or Mevastatin, indicating that those statins show high selectivity toward tumor cells (Fig. 1B-E).

3.2. SAHA and Simvastatin have synergistic effects on TNBC cells

Combination index (CI) was introduced as the standard measurement of efficacy in combination that indicates a greater (CI < 1), lesser (CI > 1) or similar (CI = 1) effect than the expected additive effect. We performed CI determination in four TNBC cells, and revealed significant synergism of SAHA and Simvastatin in these cells. The Dose-Effect and Effect-CI curves were shown in Fig. 2A–D, and the CI values for combination between SAHA and Simvastatin were less than 1 in all of the tested cancer cells, indicating that SAHA and Simvastatin had synergistic effect in TNBC cells (Table 3).

3.3. SAHA and Simvastatin induce apoptosis

Since SAHA in combination with Simvastatin dramatically inhibited the growth of TNBC cells. It is necessary to explore the way of cell death. We performed FACS analysis, and revealed that, Annexin-V positive apoptotic MDA-MB-231 and MDA-MB-468 cells were slightly increased after either SAHA or Simvastatin treatment, but significantly

X. Kou et al.
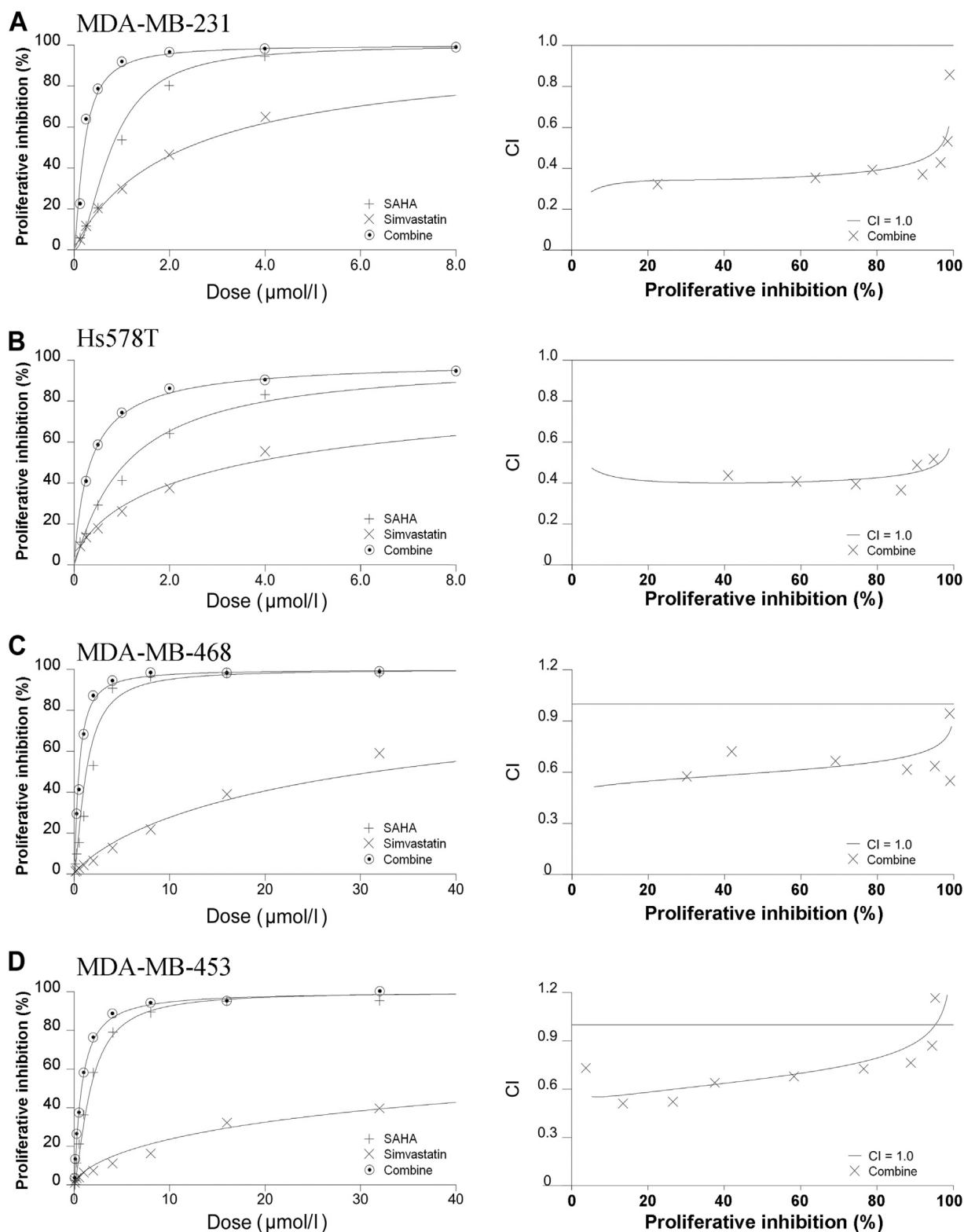
Fig. 2. SAHA and Simvastatin had synergism in inhibiting the proliferation of TNBC cells. (A) MDA-MB-231, (B) Hs578T, (C) MDA-MB-468, and (D) MDA-MB-453 cells were treated with SAHA and/or Simvastatin. Serial 2-fold dilutions of each compound in a final concentration range of 32–0.03 μmol/l were used in experiments. Cell counting was assessed by using CCK8 reagent 72 h after treatments. Dose-Effect curves and Effect-CI (combination index) curves were plotted by using software Calcusyn 2.0 (Biosoft). Experiments were performed in triplicate.

and tremendously increased by SAHA plus Simvastatin treatments (Fig. 3A and B).

When apoptosis starts, Caspase 8, 3, and 9 are cleaved and activated, resulting in the cleavage of PARP and Bid proteins. Consistent with the result of FACS, the levels of cleaved proteins were significantly increased in combination group than that with either SAHA or Simvastatin alone. However, Bcl-2, Bcl-xL, and Bax were not influenced by treatments (Fig. 3C and D).

Table 3
Combination index (CI) of SAHA and Simvastatin for inhibiting the proliferation of TNBC cells.

	MDA-MB-231	Hs578T	MDA-MB-468	MDA-MB-453
ED_{25}	0.37 ± 0.02	0.39 ± 0.02	0.56 ± 0.03[a,c]	0.49 ± 0.03[a,c]
ED_{50}	0.38 ± 0.03	0.44 ± 0.03	0.63 ± 0.03[b,c]	0.62 ± 0.04[b,c]
ED_{75}	0.40 ± 0.03	0.50 ± 0.03	0.71 ± 0.04[b,c]	0.78 ± 0.04[b,d]
ED_{90}	0.42 ± 0.03	0.58 ± 0.04	0.80 ± 0.03[b,c]	0.88 ± 0.04[b,d]

MDA-MB-231, Hs578T, MDA-MB-468, and MDA-MB-453 cells were treated with SAHA and/or Simvastatin. Serial 2-fold dilutions of each compound in a final concentration range of 32–0.03 μmol/l were used in experiments. Cell counting was assessed by using CCK8 reagent 72 h after treatments. Combination index (CI) was calculated by software Calcusyn 2.0 (Biosoft). Experiments were performed in triplicate, and data were presented as the mean ± S.E.M. Statistical analysis was performed by using one-way ANOVA.

[a] $P < 0.05$.
[b] $P < 0.01$ as compared with MDA-MB-231 cells.
[c] $P < 0.05$.
[d] $P < 0.01$ as compared with Hs578T cells.

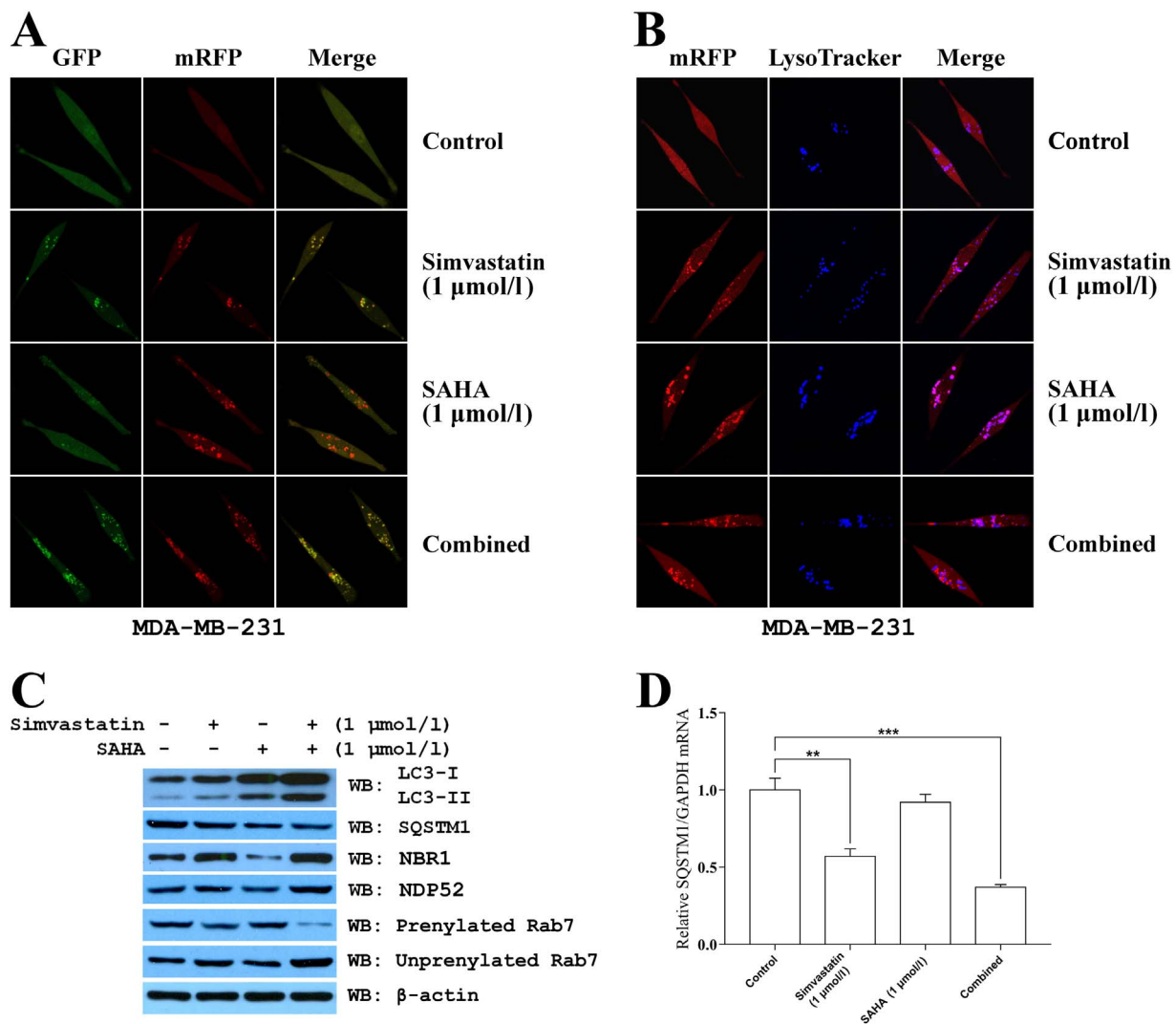### 3.4. Simvastatin obstructs autophagy initiated by SAHA

To test whether Simvastatin promotes the antitumor potential of SAHA via preventing autophagy induced by SAHA, MDA-MB-231 cells stably expressing tfLC3 were employed for the following research. tfLC3 is a pH-sensitive tandem fluorescent fusion protein consisting of monomeric red fluorescent protein (mRFP), monomeric green fluorescent protein (mGFP) and microtubule-associated protein 1 (LC3). Degradative autophagic vacuoles emit only red fluorescence, since red signal releasing mRFP resistant to the lysosomal environment; while green signal derived from eGFP is quenched in acidic and degradative amphisomes and autolysosomes environments after autophagosome-lysosome fusion; nevertheless, in initial autophagic vacuoles, tfLC3 presents both green and red, with yellow color after merge (Fujiwara et al., 2013). Our results elicited that SAHA increased autophagic flux, as shown by decrease in GFP puncta and increase in RFP puncta. Strikingly, when combined with Simvastatin, yellow puncta, increased, indicating that the co-administration could block the autophagosome-lysosome fusion to inhibit autophagic flux (Fig. 4A).

Co-localization of autophagosome and lysosome were also tested under distinct treatments. Autophagosome was tracked by mRFP-LC3, and lysosome was tagged by LysoTracker Blue. After SAHA treatment, more autophagosomes (red puncta) and lysosomes (blue) were co-localized. Simvastatin either alone or with SAHA effectively blocked the fusion of autophagosome and lysosome (Fig. 4B). By determining autophagy-related proteins, we found that SAHA induced autophagy, as evidenced by induced LC3-II and lessened SQSTM1/p62, NBR1, and NDP52 (Fig. 4C). Simvastatin obstructed autophagic flux either in basal or SAHA induced autophagy, since LC3-II, NBR1, and NDP52 were accumulated. However, Simvastatin also reduced the level of SQSTM1. To solve this discrepancy, we performed qPCR analysis of the
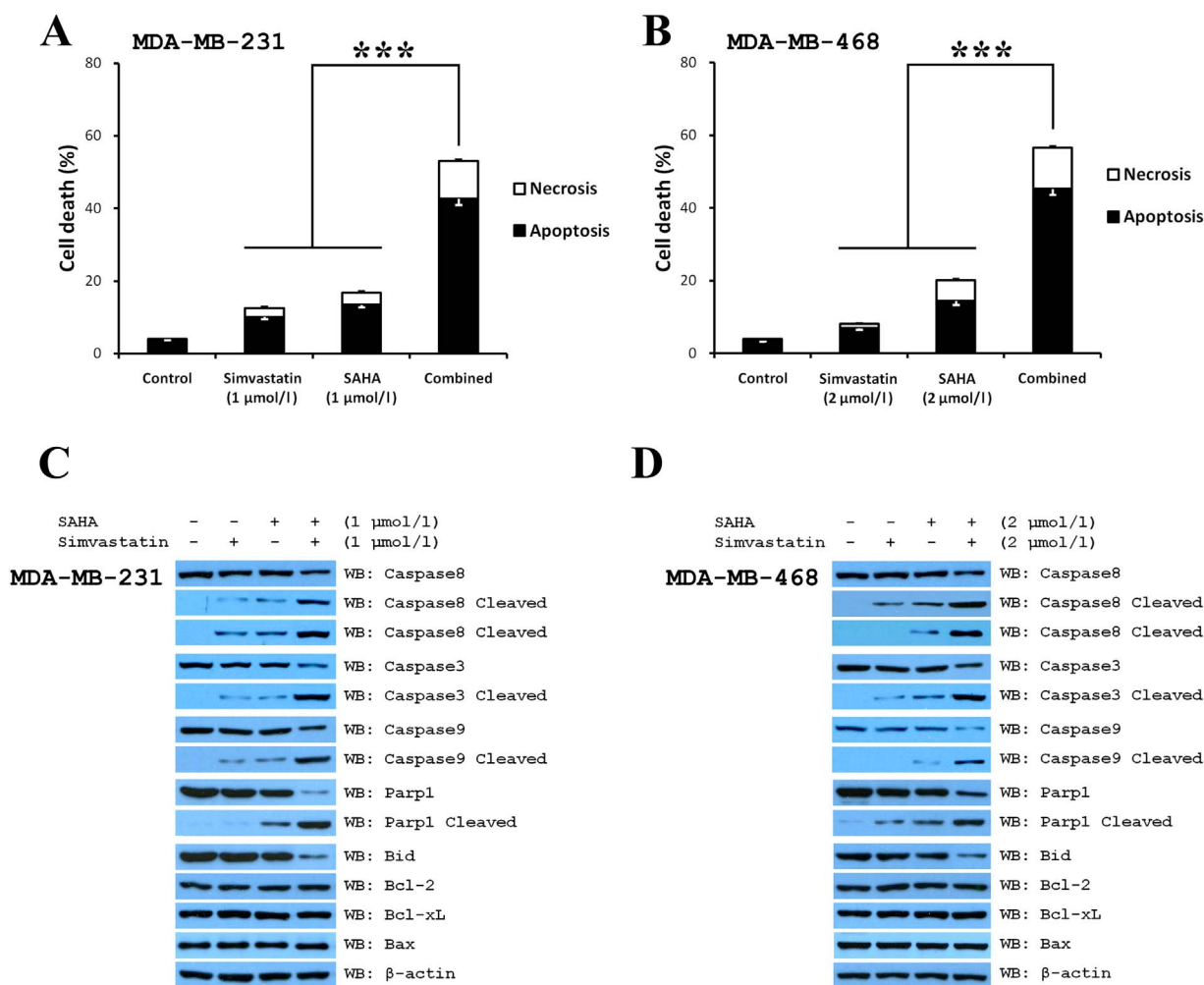
Fig. 3. SAHA and Simvastatin had synergism in inducing apoptosis against MDA-MB-231 and MDA-MB-468 cells. The apoptosis rates were determined in (A) MDA-MB-231 and (B) MDA-MB-468 cells by flow cytometry. The apoptosis-related proteins were also analyzed in (C) MDA-MB-231 and (D) MDA-MB-468 cells by Western blotting. All compounds used in MDA-MB-231 were 1 μmol/l, and in MDA-MB-468 were 2 μmol/l. Cells were treated by compounds for 24 h, and subjected to subsequent analysis.

Fig. 4. Simvastatin obstructed autophagic flux induced by SAHA in MDA-MB-231. MDA-MB-231 cells that stable expressing (A) tfLC3 or (B) mRFP-LC3 were analyzed by confocal microscopy. MDA-MB-231 cells were treated with SAHA (1 μmol/l) and/or Simvastatin (1 μmol/l) for 16 h. Representative fluorescence images are shown. (C) Immunoblotting analysis of autophagy-related proteins. (D) Relative SQSTM1/GAPDH mRNA ratio was analyzed in MDA-MB-231 cells by qPCR. Experiments were performed in triplicate, and data were presented as mean ± S.E.M. Statistical analysis was performed by using one-way ANOVA. **$P < 0.01$, ***$P < 0.001$ as compared with vehicle treatment.

transcription of SQSTM1 and found that Simvastatin could significantly reduce the mRNA level of SQSTM1 (Fig. 4**D**).

### 3.5. Simvastatin has synergism with SAHA by targeting Rab7 to interrupt autophagic flux

To determine whether the inhibition of autophagosome-lysosome fusion promoted apoptosis in MDA-MB-231 cells, Bafilomycin A (BAF-A), an inhibitor of autophagosome-lysosome fusion (Moon et al., 2015), was supplemented with distinct agents. BAF-A showed synergistic effect with SAHA on apoptosis in MDA-MB-231, but its effect was not promoted when combined with Simvastatin. Chloroquine (CQ), another inhibitor of autophagic flux by impairing acidification in lysosome lumen (Moon et al., 2015), could also boost the apoptotic effect induced by SAHA; however, had little synergism with Simvastatin or SAHA plus Simvastatin (Fig. 5**A**). BAF-A or CQ had no influence on Rab7 prenylation in MDA-MB-231 (Fig. 5**B**), implying the function of these compounds was via inhibiting Rab7 prenylation. Interestingly, BAF-A or CQ could substantially obstruct the autophagic flux initiated by SAHA, but only slightly enhanced the obstruction on autophagic flux induced by Simvastatin in MDA-MB-231 cells (Fig. 5**B**).

To further address the relationship between obstructed autophagic

flux and enhanced apoptosis in cells, we employed bioinformatics to search targets that might affect autophagosome-lysosome fusion. Rab7, a member of small GTPases, is reported to be responsible for autophagy maturation (Zhou et al., 2016), governing microtubule minus-end as well as plus-end directed transport and facilitating the fusion of autophagososme with lysosome (Wang et al., 2011; Wen et al., 2017). Importantly, Rab7 could be prenylated at 205 and 207 cysteine residues (Wu et al., 2009). As shown in Fig. 4**C** and Fig. 5**B**, **D**, and **F**, treatments with Simvastatin, an inhibitor of mevalonate pathway resulted in a significantly reduced prenylation on Rab7 in cells, proving that the autophagy maturation was blocked as observed in Fig. 4**A** and **B**.

Cells over-expressing wild type or inactive Rab7 were also tested for cell death after treatments. Cells over-expressing wild type, but not inactive Rab7 were resistant to Simvastatin treatment indicating that Rab7 was involved in the autophagosome-lysosome fusion inhibited by Simvastatin (Fig. 5**C**). Moreover, wild type, but not inactive Rab7 could restore the compromised autophagic flux inhibited by Simvastatin-containing treatments in MDA-MB-231 (Fig. 5**D**).

At last, cells were pretreated with mevalonate before incubating with testing compounds to rescue the apoptosis of cells. Mevalonate (250 μmol/l) could lessen the apoptosis ratio to nearly half of that in combination treatment (Fig. 5**E**). The prenylation of Rab7 and

X. Kou et al.
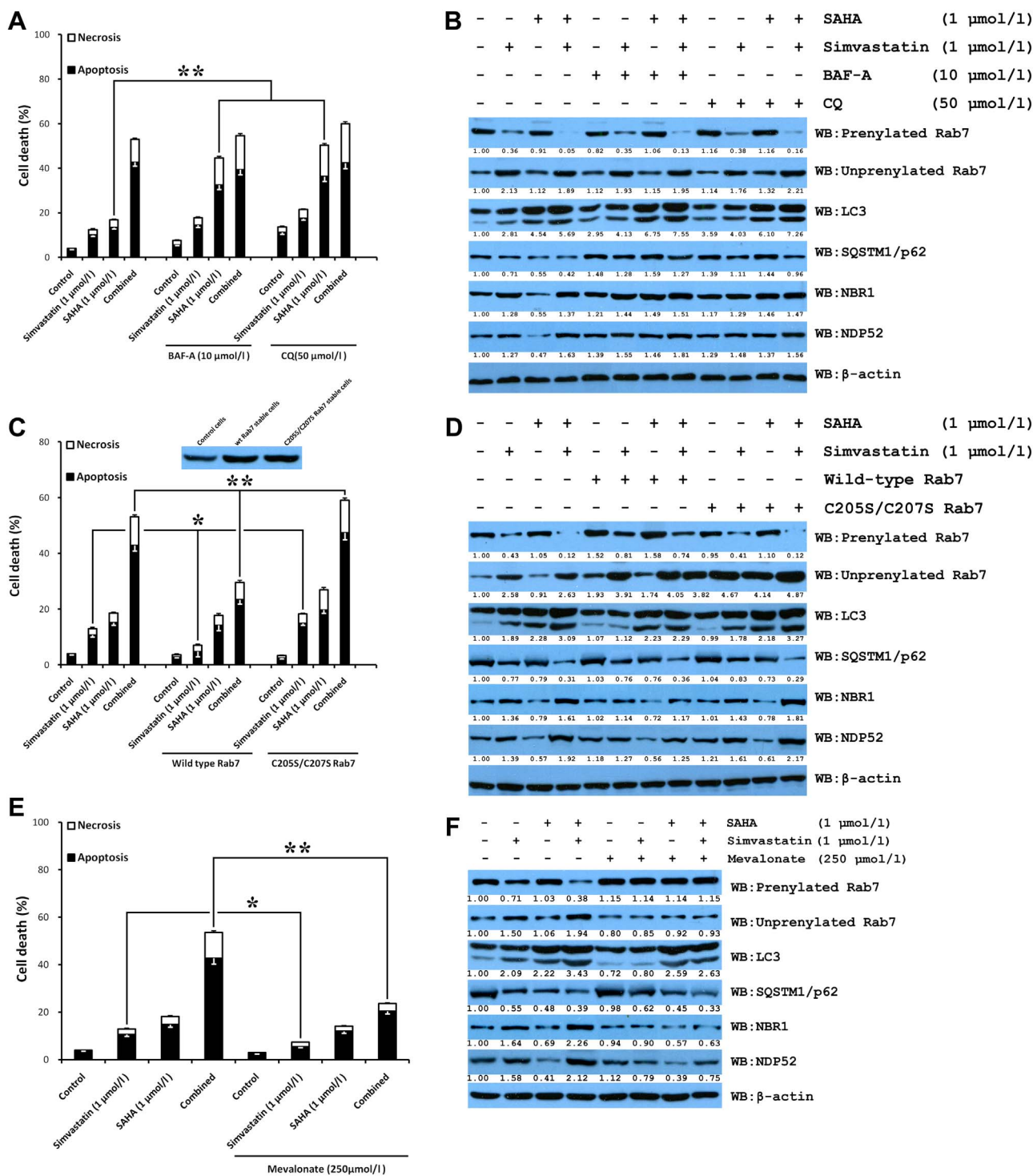
Fig. 5. SAHA and Simvastatin have synergism in inducing apoptosis against cancer cells by targeting Rab7 to inhibit autophagosome-lysosome fusion. (A) Autophagosome-lysosome fusion inhibitor Bafilomycin A (BAF-A) or Chloroquine (CQ) have synergism with SAHA, but not with Simvastatin-containing treatments in inducing apoptosis in MDA-MB-231. (B) The influence of BAF-A or CQ on the Rab7 prenylation and autophagy after SAHA and/or Simvastatin treatments in MDA-MB-231 cells. BAF-A or CQ had no influence on Rab7 prenylation in MDA-MB-231. BAF-A or CQ could substantially obstruct the autophagic flux initiated by SAHA, but only slightly enhanced the obstruction on autophagic flux induced by Simvastatin in MDA-MB-231. MDA-MB-231 cells were pretreated with 10 µmol/l BAF-A or 50 µmol/l CQ 4 h before testing compounds. (C) MDA-MB-231 cells over-expressing wild type, but not inactive (C205S/C207S double mutation) Rab7 were resistant to Simvastatin with or without SAHA treatment. (D) Wild type, but not inactive Rab7 could restore the compromised autophagic flux induced by Simvastatin in MDA-MB-231. (E) Mevalonate could lessen the apoptosis induced by Simvastatin with or without SAHA treatment in MDA-MB-231 cells. (F) Mevalonate could restore the obstructed Rab7 prenylation and autophagy induced by Simvastatin in MDA-MB-231 cells. MDA-MB-231 cells were pretreated with 250 µmol/l mevalonate 4 h before testing compounds. Apoptosis detections were performed by flow cytometry. The final concentrations of SAHA and Simvastatin used in MDA-MB-231 were 1 µmol/l. Cells were treated by testing compounds for 24 h, and subjected to subsequent analysis. Experiments were performed in triplicate, and data were presented as mean ± S.E.M. Statistical analysis was performed in experiments A and E by using one-way ANOVA, and in experiment C by using two-way ANOVA. $*P < 0.05$, $**P < 0.01$ as compared with vehicle treatment.
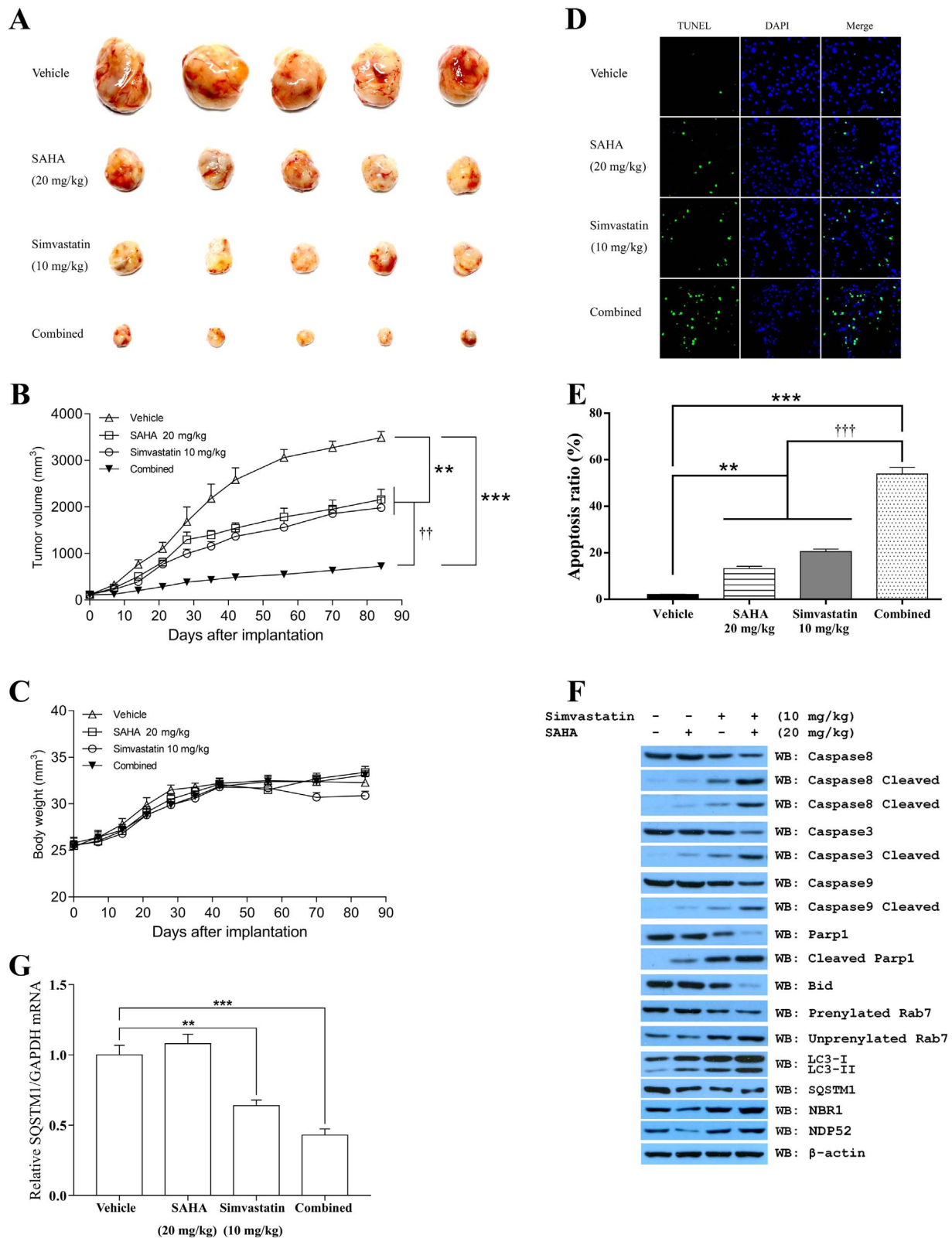
Fig. 6. SAHA and Simvastatin have synergism in inhibiting tumor growth in MDA-MB-231 cells xenografted mice. (A) Photographs of subcutaneous tumors resulting from indicated treatments in xenografted mice. (B) Tumor growth curves and (C) body weight curves during treatments with compounds in xenografted mice. (D) Detection of apoptosis by TUNEL assay in five different views of each tumor slice by confocal microscopy. Green fluorescence indicates apoptotic (TUNEL positive) cells, and nuclei of tumor cells were stained with DAPI (blue fluorescence). (E) Quantitative evaluation of apoptotic cells. The apoptotic ratio was calculated by counts of green fluorescence versus that of blue fluorescence. (F) Immunoblotting analysis of xenograft tumor tissues. (G) Relative SQSTM1/GAPDH mRNA ratio was analyzed in tumor tissue by qPCR. Tumor-bearing mice were treated with vehicle, Simvastatin (10 mg/kg/day, orally), SAHA (20 mg/kg/day, orally), or their combination. Data were presented as mean ± S.E.M. (five samples in each group). Statistical analysis was performed by using one-way ANOVA. $**P < 0.01$, $***P < 0.001$ as compared with vehicle treatment. $^{††}P < 0.01$ as compared with either SAHA or Simvastatin treatment alone.

compromised autophagy were also restored by mevalonate supplementation (Fig. 5**F**).

3.6. SAHA and Simvastatin inhibit tumor growth in MDA-MB-231 xenografted mice

Tumor-bearing mice were treated with vehicle, Simvastatin (10 mg/kg/day), SAHA (10 mg/kg/day), or there combination. SAHA plus Simvastatin was more potent in inhibiting tumor growth compared with either alone (Fig. 6**A**). The final average tumor volume in SAHA plus Simvastatin group were 728 mm^3, in comparison with control (3492 mm^3), SAHA alone (2161 mm^3), and Simvastatin alone (1986 mm^3) (Fig. 6**B**). The dosage of compounds used in this study did not lead to obvious toxicity (Fig. 6**C**). TUNEL staining showed $2.12 \pm 0.21\%$ apoptosis in tumor from control group, $13.24 \pm 0.98\%$ in tumor from Simvastatin group, $20.52 \pm 1.14\%$ in tumor from SAHA group, and $53.90 \pm 2.78\%$ in tumors from combination group (Fig. 6**D** and **E**). Finally, we detected prenylated and unprenylated Rab7, Caspase 8, Caspase 3, Caspase 9, PARP1, and Bid in tumor samples. Consistent with results obtained from cultured cells, SAHA plus Simvastatin treatment obstructed Rab7 prenylation and autophagy (Fig. 6**F**), and thus enhanced cleavage of Caspase 8, 3, and 9, and further the cleavage of PARP1 and Bid, indicating the activated apoptosis cascade (Fig. 6**F**). Similar with cell-based results, Simvastatin could induce accumulations on LC3-II, NBR1, and NDP52, but lead to attenuation on the transcription of SQSTM1 (Fig. 6**G**).

4. Discussion

TNBC is a subset of breast cancer defined by the absence of ER, PR, and HER2, and represents a panel of heterogeneous tumors based on gene-expressing profiling (Lehmann et al., 2011). Despite great efforts were made in adjuvant chemotherapy regimens, the overall survival and prognosis for patients with TNBC is significantly lower than those who with either ER$^+$ or HER2$^+$ breast cancers (Bianchini et al., 2016). New treatment strategies are needed for patients with TNBC emergently. SAHA inhibits Class I and II HDACs, and thus increased the expression of some tumor-repressing genes to exert antitumor efficiency. However, SAHA administration alone is not potent enough to overcome TNBC. Supplementation with other agents may be better choices. By screening LOPAC library, we found that SAHA and Mevastatin have synergistic effect on TNBC cells. Because of severe adverse effect, Mevastatin did not enter into clinic, but its analogue Simvastatin and Pravastatin have been using for more than decades. Simvastatin, but not Pravastatin promotes the antitumor potency of SAHA.

SAHA increases the expression of some tumor-repressing genes by epigenetic dependent and/or independent pathways and induces tumor apoptosis (Grant et al., 2007; Haas et al., 2014; Schelman et al., 2013; West and Johnstone, 2014). It also induces autophagy that can neutralize its antitumor potential. Compounds inhibiting autophagy may have synergism with SAHA. Simvastatin is a potent inhibitor to HMGCR that catalyzes the rate-limiting step in cholesterol biosynthesis through the endogenous mevalonate cascade. Not only the synthesis of cholesterol, but also that of other by-products can be inhibited by Simvastatin, including the mevalonate and downstream isoprenoids, such as farnesyl and geranylgeranyl groups (Woschek et al., 2016). These isoprenoids can be attached to some special proteins anchoring to membrane inside cells and exert their biological functions (Wu et al., 2009). Among them, Rab7 is involved in autophagosome-lysosome fusion. By inhibiting HMGCR, Simvastatin deprives the source of isoprenoids, prevents the prenylation of Rab7, and reduces its roles in autophagosome-lysosome fusion. The involvement of Rab7 inhibition in promoted apoptosis by compounds is further evidenced by a series of experiments.

Firstly, autophagic flux inhibitor BAF-A and CQ enhanced the pro-apoptotic effect of SAHA, but could not further increase that induced by

Simvastatin. To better reveal the target of Simvastatin, we focused on Rab7, a critical player mediating the fusion between autophagosome and lysosome. Over-expression of wild-type, but not inactive Rab7 could compromise the synergism of SAHA and Simvastatin. We deduced that over-expressed Rab7 competed for the prenylation with other proteins to accumulate enough functional Rab7 and restore the interrupted autophagic flux. At last, exogenously supplied mevalonate could decrease the apoptosis induced by Simvastatin, but not that by SAHA treatment alone. Meanwhile, the rescue effect could be observed along with the restoration of Rab7 prenylation.

To further confirm that the combination of SAHA and Simvastatin could have potential clinical significance, we evaluated their antitumor activity in MDA-MB-231 xenografted mice. As expected, combination could significantly and dramatically attenuate the tumor growth in mice. The antitumor potency by combination was much stronger than that by either alone. The apoptosis in tumor and Rab7 prenylation were enhanced by Simvastatin.

The relative safety of Simvastatin has led to the conversation from prescription to over-the-counter medicine in the UK (Forde et al., 2011). The relatively low of charge in Simvastatin administration makes it a good candidate for cancer treatment. In this study we described for the first time that SAHA and Simvastatin could have synergism in inhibiting TNBC cells. We also revealed the mechanisms underlying this combination. As a preliminary of series, subsequent researches focusing on strategies to further enhance the efficacy are carrying out.

References

Åberg, M., Wickström, M., Siegbahn, A., 2008. Simvastatin induces apoptosis in human breast cancer cells in a NFκB-dependent manner and abolishes the anti-apoptotic signaling of TF/FVIIa and TF/FVIIa/FXa. Thromb. Res. 122, 191–202.

Bianchini, G., Balko, J.M., Mayer, I.A., Sanders, M.E., Gianni, L., 2016. Triple-negative breast cancer: challenges and opportunities of a heterogeneous disease. Nat. Rev. Clin. Oncol. 13, 674–690.

Blows, F.M., Driver, K.E., Schmidt, M.K., Broeks, A., van Leeuwen, F.E., 2010. Subtyping of breast cancer by immunohistochemistry to investigate a relationship between subtype and short and long term survival: a collaborative analysis of data for 10,159 cases from 12 studies. PLoS Med. 7, e1000279.

Chiu, H.W., Yeh, Y.L., Wang, Y.C., Huang, W.J., Ho, S.Y., Lin, P., 2016. Combination of the novel histone deacetylase inhibitor YCW1 and radiation induces autophagic cell death through the downregulation of BNIP3 in triple-negative breast cancer cells in vitro and in an orthotopic mouse model. Mol. Cancer 15, 46.

Deming, D.A., Ninan, J., Bailey, H.H., Kolesar, J.M., Eickhoff, J., Reid, J.M., 2014. A Phase I study of intermittently dosed vorinostat in combination with bortezomib in patients with advanced solid tumors. Investig. New Drugs 32, 323–329.

Dupere-Richer, D., Kinal, M., Menasche, V., Nielsen, T.H., Del Rincon, S., Pettersson, F., 2013. Vorinostat-induced autophagy switches from a death-promoting to a cyto-protective signal to drive acquired resistance. Cell Death Dis. 4, e486.

Forde, I., Chandola, T., Raine, R., Marmot, M.G., Kivimaki, M., 2011. Socioeconomic and ethnic differences in use of lipid-lowering drugs after deregulation of simvastatin in the UK: the Whitehall II prospective cohort study. Atherosclerosis 215, 223–228.

Fujiwara, E., Washi, Y., Matsuzawa, T., 2013. Observation of autophagosome maturation in the interferon-gamma-primed and lipopolysaccharide-activated macrophages using a tandem fluorescent tagged LC3. J. Immunol. Methods 394, 100–106.

Gandesiri, M., Chakilam, S., Ivanovska, J., Benderska, N., Ocker, M., Di Fazio, P., 2012. DAPK plays an important role in panobinostat-induced autophagy and commits cells to apoptosis under autophagy deficient conditions. Apoptosis 17, 1300–1315.

Giuliano, A.E., Connolly, J.L., Edge, S.B., Mittendorf, E.A., Rugo, H.S., Solin, L.J., 2017. Breast Cancer-major changes in the American joint committee on cancer eighth edition cancer staging manual. CA Cancer J. Clin. http://dx.doi.org/10.3322/caac.21393.

Gopalan, A., Yu, W., Sanders, B.G., Kline, K., 2013. Simvastatin inhibition of mevalonate pathway induces apoptosis in human breast cancer cells via activation of JNK/CHOP/DR5 signaling pathway. Cancer Lett. 329, 9–16.

Grant, S., Easley, C., Kirkpatrick, P., 2007. Vorinostat. Nat. Rev. Drug Discov. 6, 21–22.

Haas, N.B., Quirt, I., Hotte, S., McWhirter, E., Polintan, R., Litwin, S., 2014. Phase II trial of vorinostat in advanced melanoma. Investig. New Drugs 32, 526–534.

Lehmann, B.D., Bauer, J.A., Chen, X., Sanders, M.E., Chakravarthy, A.B., Shyr, Y., 2011.

Identification of human triple-negative breast cancer subtypes and preclinical models for selection of targeted therapies. J. Clin. Investig. 121, 2750–2767.

Moon, E.K., Kim, S.H., Hong, Y., Chung, D.I., Goo, Y.K., Kong, H.H., 2015. Autophagy inhibitors as a potential antiamoebic treatment for Acanthamoeba keratitis. Antimicrob. Agents Chemother. 59, 4020–4025.

Mowers, E.E., Sharifi, M.N., Macleod, K.F., 2016. Novel insights into how autophagy regulates tumor cell motility. Autophagy 12, 1679–1680.

Palmieri, D., Lockman, P.R., Thomas, F.C., Hua, E., Herring, J., Hargrave, E., 2009. Vorinostat inhibits brain metastatic colonization in a model of triple-negative breast cancer and induces DNA double-strand breaks. Clin. Cancer Res. 15, 6148–6157.

Patel, S., Hurez, V., Nawrocki, S., Goros, M., Michalek, J., 2016. Vorinostat and hydroxychloroquine improve immunity and inhibit autophagy in metastatic colorectal cancer. Oncotarget 13, 59087–59097.

Schech, A., Kazi, A., Yu, S., Shah, P., Sabnis, G., 2015. Histone deacetylase inhibitor entinostat inhibits tumor-initiating cells in triple-negative breast cancer cells. Mol. Cancer Ther. 14, 1848–1857.

Schelman, W.R., Traynor, A.M., Holen, K.D., Kolesar, J.M., Attia, S., Hoang, T., 2013. A phase I study of vorinostat in combination with bortezomib in patients with advanced malignancies. Investig. New Drugs 31, 1539–1546.

Tate, C., Rhodes, L., Segar, H., Driver, J.L., Pounder, F., Burow, M., 2012. Targeting triple-negative breast cancer cells with the histone deacetylase inhibitor panobinostat. Breast Cancer Res. 14, R79.

Torgersen, M.L., Engedal, N., Boe, S.O., Hokland, P., Simonsen, A., 2013. Targeting autophagy potentiates the apoptotic effect of histone deacetylase inhibitors in t(8;21)

AML cells. Blood 122, 2467–2476.

Wang, T., Ming, Z., Xiaochun, W., Hong, W., 2011. Rab7: role of its protein interaction cascades in endo-lysosomal traffic. Cell Signal. 23, 516–521.

Wei, H., Wang, C., Croce, C.M., Guan, J.L., 2014. p62/SQSTM1 synergizes with autophagy for tumor growth in vivo. Genes Dev. 28, 1204–1216.

Wen, H., Zhan, L., Chen, S., Long, L., Xu, E., 2017. Rab7 may be a novel therapeutic target for neurologic diseases as a key regulator in autophagy. J. Neurosci. Res. http://dx.doi.org/10.1002/jnr.24034.

West, A.C., Johnstone, R.W., 2014. New and emerging HDAC inhibitors for cancer treatment. J. Clin. Investig. 124, 30–39.

Woschek, M., Kneip, N., Jurida, K., Marzi, I., Relja, B., 2016. Simvastatin reduces cancerogenic potential of renal cancer cells via geranylgeranyl pyrophosphate and mevalonate pathway. Nutr. Cancer 68, 420–427.

Wu, Y., Goody, R., Abagyan, R., Alexandrov, K., 2009. Structure of the disordered C terminus of Rab7 GTPase induced by binding to the Rab geranylgeranyl transferase catalytic complex reveals the mechanism of Rab prenylation. J. Biol. Chem. 284, 13185–13192.

Zhou, T., Jin, M., Ding, Y., Zhang, Y., Sun, Y., Huang, S., 2016. Hepatitis B virus dampens autophagy maturation via negative regulation of Rab7 expression. Biosci. Trends 10, 244–250.

Zibelman, M., Wong, Y.N., Devarajan, K., Malizzia, L., Corrigan, A., Olszanski, A.J., 2015. Phase I study of the mTOR inhibitor ridaforolimus and the HDAC inhibitor vorinostat in advanced renal cell carcinoma and other solid tumors. Investig. New Drugs 33, 1040–1047.